Water Research 130 (2018) 31–37

Contents lists available at ScienceDirect

Water Research

journal homepage: www.elsevier.com/locate/watres

Inactivation kinetics and efficiencies of UV-LEDs against *Pseudomonas aeruginosa*, *Legionella pneumophila*, and surrogate microorganisms

Surapong Rattanakul, Kumiko Oguma*

Research Center for Advanced Science and Technology, The University of Tokyo, 4-6-1 Komaba, Meguro-ku, Tokyo 153-8904, Japan

ARTICLE INFO

Article history:
Received 1 August 2017
Received in revised form
18 November 2017
Accepted 23 November 2017
Available online 23 November 2017

Keywords:
UV light-emitting diode
Disinfection
Inactivation rate constant
Energy efficiency
Water treatment

ABSTRACT

To demonstrate the effectiveness of UV light-emitting diodes (UV-LEDs) to disinfect water, UV-LEDs at peak emission wavelengths of 265, 280, and 300 nm were adopted to inactivate pathogenic species, including *Pseudomonas aeruginosa* and *Legionella pneumophila*, and surrogate species, including *Escherichia coli*, *Bacillus subtilis* spores, and bacteriophage Qβ in water, compared to conventional low-pressure UV lamp emitting at 254 nm. The inactivation profiles of each species showed either a linear or sigmoidal survival curve, which both fit well with the Geeraerd's model. Based on the inactivation rate constant, the 265-nm UV-LED showed most effective fluence, except for with *E. coli* which showed similar inactivation rates at 265 and 254 nm. Electrical energy consumption required for 3-$\log_{10}$ inactivation ($E_{E,3}$) was lowest for the 280-nm UV-LED for all microbial species tested. Taken together, the findings of this study determined the inactivation profiles and kinetics of both pathogenic bacteria and surrogate species under UV-LED exposure at different wavelengths. We also demonstrated that not only inactivation rate constants, but also energy efficiency should be considered when selecting an emission wavelength for UV-LEDs.

1. Introduction

Ultraviolet light-emitting diodes (UV-LEDs) are small, mercury-free devices with a flexible and adjustable design. UV-LEDs can be used without a warming up period, enabling diverse application of this device such as on-demand operation. The effectiveness of UV-LEDs at various wavelengths for water disinfection has been demonstrated in many studies, with most studies investigating surrogate microorganisms such as the indicator bacterium *Escherichia coli*; indicator viruses such as bacteriophage MS2, Qβ, and T7; and aerobic spore-forming bacteria (Bowker et al., 2011; Oguma et al., 2015; Beck et al., 2017).

For example, *E. coli* inactivation by UV-LEDs with wavelengths varying from 255 to 280 nm exhibit a range of inactivation rate constants between 0.29 and 0.42 cm^2/mJ, which are comparable to the values found at 254 nm (Chatterley and Linden, 2010; Bowker et al., 2011; Oguma et al., 2013). In contrast, MS2 as a common surrogate for enteric viruses showed different sensitivities to different UV-LEDs wavelengths, and the effectiveness at 260 nm was better than that using a 254-nm low-pressure UV lamp (LPUV) at the same dose (Beck et al., 2017). Although MS2 is commonly used in North America for UV system validation in drinking water treatment plants and UV studies (USEPA, 2006), *Bacillus subtilis* spores are more widely used in Europe (ÖNORM, 2001). Moreover, because similar behaviors of aerobic spores (e.g. *B. subtilis* spores) and *Cryptosporidium* oocysts such as resistance and removal in water treatment processes have been observed (Facile et al., 2000; Muhammad et al., 2008), *B. subtilis* spores has been proposed to be as a conservative surrogate of *Cryptosporidium* to identify drinking water contamination. Although UV-LEDs were shown to be effective against surrogate microorganisms, information regarding the effectiveness of UV-LEDs against pathogenic microorganisms is very limited. Only two recent studies have reported the sensitivity of UV-LEDs on a pathogenic virus, an adenovirus known to be the most UV-resistant species (Oguma et al., 2015; Beck et al., 2017), but there have been no studies on pathogenic bacteria or protozoa in water. Because of health risk to humans posed by these microorganisms, it is necessary to examine the effectiveness of UV-LEDs against pathogenic bacteria and protozoa.

Pseudomonas aeruginosa, an opportunistic bacterium, is sometimes detected in drinking water pipeline systems because of its ability to form biofilms with extracellular polymeric substances.

* Corresponding author.
E-mail address: oguma@env.t.u-tokyo.ac.jp (K. Oguma).

https://doi.org/10.1016/j.watres.2017.11.047
0043-1354/

Abbreviations

ATCC	American Type Culture Collection
BCYE-α	buffered charcoal yeast extract supplemented with alpha-ketoglutarate
B. subtilis	*Bacillus subtilis*
CFU	colony-forming unit
CDC	Centers for Disease Control and Prevention
E. coli	*Escherichia coli*
IFO	Institute of Fermentation
L. pneumophila	*Legionella pneumophila*
LPUV	low-pressure UV lamp
ÖNORM	Österreichisches normungsinstitut
P. aeruginosa	*Pseudomonas aeruginosa*
PBS	phosphate-buffered solution
PFU	plaque-forming unit
RMSE	root mean square error
UV-LEDs	ultraviolet light-emitting diodes
USEPA	United States Environmental Protection Agency
WHO	World Health Organization

Biofilm formation makes it difficult for residual chlorine to diffuse and inactivate microorganisms in inner layers, and can result in re-contamination of drinking water (Meena and Gerba, 2009). Infection by *P. aeruginosa* has been reported following intake of contaminated drinking water, and serious infection cases are predominantly found in hospitals, resulting in pneumonia, bloodstream infections, urinary tract infections, and surgical site infections. The Centers for Disease Control and Prevention (CDC) in the United States reported 51,000 infections of *P. aeruginosa* per year with approximately 6700 cases of multi-drug resistance resulting in 400 deaths per year (CDC, 2013). As a result, the World Health Organization (WHO) has listed *P. aeruginosa* as a critical priority (WHO, 2017). Similarly, *Legionella pneumophila*, another water-borne pathogen that thrives in biofilms, was reported to account for 66% of drinking water-associated outbreaks in 2011–2012 (CDC, 2015). Legionnaires' disease has a fatality rate of approximately 30% among healthcare-associated cases and the risk is particularly high for elderly people (Demirjian et al., 2015). Therefore, it is challenging to find solutions for Legionnaires' disease and *P. aeruginosa* infections, and UV-LEDs may be a solution for controlling these important causative agents of healthcare-associated infections at point-of-entry or point-of-use of water, particularly in hospitals.

The objective of this study was to investigate the efficiency of both inactivation and energy consumption of UV-LEDs at various wavelengths for the following pathogens: *P. aeruginosa*, *L. pneumophila*, and surrogate microorganisms, including *E. coli*, bacteriophage Qβ, and *B. subtilis* spores. We aimed to offer supporting information for the selection of UV-LED wavelength, which is valuable for future development of water disinfection systems equipped with UV-LEDs.

2. Materials and methods

2.1. Cultivation and enumeration of microorganisms

Surrogate microorganisms, including *E. coli* IFO 3301 (Institute for Fermentation, Japan), *B. subtilis* spores ATCC 6633 (American Type Culture Collection (ATCC), Manassas, VA, USA), and bacteriophage Qβ ATCC 15597 B1 (ATCC), were cultivated as follows.

Escherichia coli. A pure culture of *E. coli* was incubated at 37 °C overnight in Luria-Bertani broth and subsequently washed with phosphate-buffered solution (PBS, pH 7.2) 3 times before the UV exposure experiments. The number of *E. coli* was determined in a colony-forming unit (CFU) assay with Chromocult agar according to the method of manufacturer (Merck, Darmstadt, Germany).

***Bacillus subtilis* spores**. Cultivation, harvesting and determination technique of *B. subtilis* spores were modified from the methods of Nicholson and Setlow (1990) in which a pure culture stock of *B. subtilis* was incubated in Trypticase soy broth at 37 °C for 6 h, transferred into liquid enrichment medium, 2 × SG medium, and then incubated at 37 °C with vigorous aeration for 7–8 days for sporulation. Subsequently, *B. subtilis* spores were harvested by washing with cold sterile water three times, heating at 80 °C for 12 min to inactivate vegetative and germinating cells, and washing again with cold sterile water 6 times sequentially. The purity of the spore solution according to phase-contrast microscopy was up to 90%. The number of active spores was determined by CFU assays with nutrient agar at 37 °C after 24 h incubation.

Bacteriophage Qβ. An aliquot (100 μL) of bacteriophage Qβ prepared and purified as described previously (Rattanakul et al., 2014) was mixed in PBS for UV exposure experiments and to enumerate Qβ. A double-layer agar technique using *E. coli* K-12 A/λ (F+) as a host was applied to Qβ-containing samples, which were evaluated as plaque-forming units (PFU) per mL (Adam, 1959).

For pathogenic microorganisms, including *L. pneumophila* ATCC 33152 and *P. aeruginosa* ATCC 10145, the details of cultivation were as follows.

***Legionella pneumophila*.** A modified method of Buse et al. (2015) for cultivation and determination of *L. pneumophila* was performed as follows. A stock solution of *L. pneumophila* was cultivated in buffered yeast extract medium at 37 °C for 48 h and then washed 3 times with PBS before use. The enumeration method was performed using a CFU assay with buffered charcoal yeast extract (BCYE-α) agar (CM0655, Oxoid, Hampshire, UK) supplied with growth supplement (SR 0110, Oxoid) at 37 °C for 4 days of incubation.

Pseudomonas aeruginosa. *Pseudomonas aeruginosa* samples were prepared by incubating an aliquot of stock solution in nutrient broth at 37 °C for 24 h and washing with PBS 3 times. Nutrient broth agar was used to measure the number of *P. aeruginosa* in a CFU assay at 37 °C and 24 h incubation following the method provided by ATCC.

2.2. Apparatuses for UV-LED, LPUV, and fluence measurement

UV-LEDs (Nikkiso Giken Co. Ltd., Ishikawa, Japan) with peak emission wavelengths of 265, 280, and 300 nm were used. The UV-LED apparatus consisted of a circuit board installed with 8 UV-LED chips in a circular arrangement for each wavelength (4 chips in series, 2 series in parallel), fan, a power supply unit, and temperature control system as shown in Fig. 1a. To set equivalent fluence rate at the surface of the microbial suspensions for different UV-LEDs, the electronic currents required for each UV-LED were 51.5 mA for 265-nm, 18.5 mA for 280-nm, and 14.5 mA for 300-nm. The voltages needed to achieve these values were 6.05 V for 265-nm, 5.16 V for 280-nm and 4.82 V for 300-nm, respectively. The fluence rate or irradiance was measured by ferrioxalate actinometry (Bolton et al., 2011) and fluence rates were 0.99 mW/cm^2 for 265- and 280-nm UV-LEDs and 1.01 mW/cm^2 for 300-nm UV-LEDs. The incident fluence rate was adjusted as described by Bolton and Linden (2003) considering water (e.g. UV absorbance and water depth) and reflection factor (only for LPUV system), and the fluence was a product of time and the incident fluence rate.

A collimated beam low-pressure UV (LPUV) system was used for

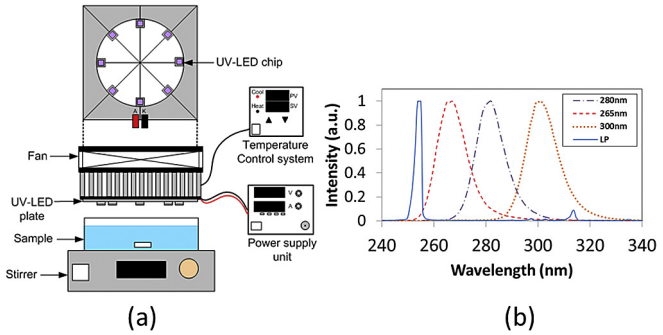

Fig. 1. (a) UV-LED setup and (b) emission spectra of UV-LEDs and LPUV.

comparison and consisted of a 15-W LPUV lamp (GL15, Toshiba, Japan) emitting a peak wavelength at 254 nm, shutter, and time controller. The fluence rate was measured using a radiometer (UVR2 UD25, TOPCON) following an adjustment method as described previously. The emission spectra of UV-LEDs and LPUV are shown in Fig. 1b.

2.3. UV disinfection procedure

Disinfection procedures for both UV-LEDs and LPUV were similar and each microorganism was tested separately as follows. Five or 35 mL of PBS spiked with microbial stock solution was placed in a glass Petri dish with diameter of 3 or 8.5 cm providing sample depth of 0.707 or 0.617 cm under the UV-LEDs or LPUV system, respectively, which was continuously stirred with a magnetic bar throughout the disinfection experiments. Untreated (N_0) and treated samples (N_t) were collected at exposure time zero and designated exposure times t; to eliminate the effects of photoreactivation, UV disinfection experiments were performed at least three independent batches with a vary of exposure time among the batches under a red light condition and all treated samples were kept in the dark until microbial analysis.

2.4. Inactivation kinetics

UV inactivation kinetics of each species at difference wavelengths was mathematically determined from fluence-response curves using a multi-target model (Severin et al., 1983) as described by the following equation:

$$\frac{N_t}{N_0} = 1 - \left(1 - 10^{-kF}\right)^{n_c} \quad (1)$$

where N_0 and N_t are the microbial concentration (CFU or PFU/mL) at time zero and t, respectively, k is the inactivation rate constant (cm^2/mJ), F is the UV fluence at exposure time t, and n_c is the number of critical targets to cause inactivation. The values of k and n_c are the slope and y-intercept of the linear region of the fluence-response curve. The multi-target model (Eq. (1)) can be reduced to a single target model, if n_c is equal to 1 as follows:

$$\frac{N_t}{N_0} = 10^{-kF} \quad (2)$$

Another inactivation kinetic model proposed by Geeraerd et al. (2000) (later expressed as the Geeraerd's model) considering effects of shoulder and tailing was applied to compare with the multi-target model, and Geeraerd's model is derived from Eq. (3).

$$\frac{N_t}{N_0} = 10^{-kF}\left(1 - \frac{N_{res}}{N_0}\right)\left(\frac{10^{kt_l}}{1 + \left(10^{k(t_l - t)} - 10^{-kt}\right)}\right) + \frac{N_{res}}{N_0} \quad (3)$$

where N_{res} is the microbial concentration of a specific subpopulation, either more resistant or appearing as a result of experimental artifacts (CFU or PFU/mL), k is the maximum inactivation rate constant of critical components, given as the slope of the linear part (cm^2/mJ), and t_l is the shoulder length (mJ/cm^2), which can be obtained by dividing the value of y-intercept of the linear part with the k.

2.5. Electrical energy efficiency

The electrical energy per order (E_{EO}) is a parameter used to assess the performance of different UV disinfection systems (i.e. UV-LEDs and LPUV) based on electrical energy consumption, which is defined as the amount of electrical energy required to lower the concentration of microbes by one order of magnitude in a specific volume of water. If the linear fluence-response profile is observed, E_{EO} can be derived as follows (Sharpless and Linden, 2005):

$$E_{EO} = \frac{A}{3.6 \times 10^3 \times V \times k \times C \times WF} \quad (4)$$

where E_{EO} is the electrical energy per order of magnitude (kWh/m^3/order), A is the irradiant surface area (cm^2), V is the volume of sample (mL), k is the fluence-based inactivation rate constant (cm^2/mJ), WF is the water factor, the value of 3.6×10^3 is a unit conversion constant for mW and kW, sec and hr, and mL and m^3, and C is the wall plug efficiency which can be calculated based on Eq. (5).

$$C = \frac{P_{output}}{P_{input}} = \frac{F_A}{I_A \times V_A} \quad (5)$$

where P_{output} is the UV-LEDs optical power (mW), P_{input} is the applied electrical power (mW), I_A is the applied current (mA), V_A is the applied voltage (V), and F_A is the radiant flux (mW). Information regarding radiant flux per UV-LED chip provided by the manufacturer (Nikkiso Giken Co. Ltd.) was 2.01 mW for 265-nm, 1.82 mW for 280-nm and 300-nm UV-LEDs. Accordingly, the C values became 0.333 for the LPUV, 0.006 for the 265-nm, 0.019 for the 280-nm, and 0.026 for the 300-nm UV-LEDs, respectively.

In cases where fluence-response curves showed non-linear log reduction (e.g. shoulder, tailing or sigmoidal curve), the electrical energy per specific n-$\log_{10}$ reduction, ($E_{E,n}$, kWh/m^3/n-log reduction) was calculated as follows (Beck et al., 2017):

$$E_{E,n} = \frac{A \times F_n}{3.6 \times 10^3 \times V \times C \times WF} \quad (6)$$

where F_n is the fluence required for n-$\log_{10}$ reduction (mJ/cm^2).

2.6. Model fitting and statistical analysis

Fit testing of the inactivation kinetic models for each microorganism was conducted using Microsoft Excel and either root mean square error (RMSE) or the coefficient of determination (R^2) was determined to assess the goodness of fit with the observed data. For non-linear fluence-response curves; such as a curve with shoulder and tailing, R^2 was not applicable because of invalidation of the R^2 assumption, and a higher R^2 indicated a better predicted value (model) fitted with the observed data. In contrast, a lower value for RMSE indicated a better fit. Analysis of covariance was introduced to indicate a difference in the inactivation rate in the linear part of

the inactivation profile at different UV wavelengths and *p*-values less than 0.05 indicated a significant difference.

3. Results and discussion

3.1. Inactivation kinetic modeling

Fluence-response curves or survival curves of target microorganisms inactivated by different UV wavelengths are shown in Fig. 2. Two types of survival curve, linear and sigmoidal curves (a curve with a shoulder and tailing), were observed in this study. The linear curve was observed for *L. pneumophila* and bacteriophage Qβ, whereas a sigmoidal curve was found for *E. coli*, *P. aeruginosa*, and *B. subtilis* spores. In sigmoidal curves, the shoulder may indicate the resynthesis rate of vital components, which reached a level higher than the destruction rate (Mossel et al., 1995), while tailing may have resulted from multiple-hit lowering inactivation efficiency and the existence of a small number of resistant sub-populations, including UV-induced and adapted resistance (Cerf, 1997). In the present study, the length of the shoulder on fluence-response curves as shown in Table 1 differed based on the microbial species and emission wavelengths, indicating that accumulation of damage or resynthesis of vital component before inactivation may differ among each microorganism, and different wavelengths resulted in different magnitudes of damage affecting the shoulder for the microorganims. For instance, the shoulder length at 254 nm was longer than that at 265 nm, but there was a clear increasing trend following exposure to longer wavelengths (280 and 300 nm) in *E. coli* and *B. subtilis* spores, showing the highest value at 300 nm. This indicates that damage resynthetic ability may be mostly supressed at 265 nm, but other unknown mechanisms may contribute to this phenomenon and it is needed to be examined in further studies. Tailing was observed after microorganisms were inactivated at approximately 4.5-log$_{10}$ inactivation at all wavelengths. These results support that resistant sub-populations were present even in pure cultures because after 4.5-log$_{10}$ inactivation, the microbial concentration remained approximately ~100–300 CFU/mL compared to original number of 10^6–10^7 CFU/mL (Cerf, 1997).

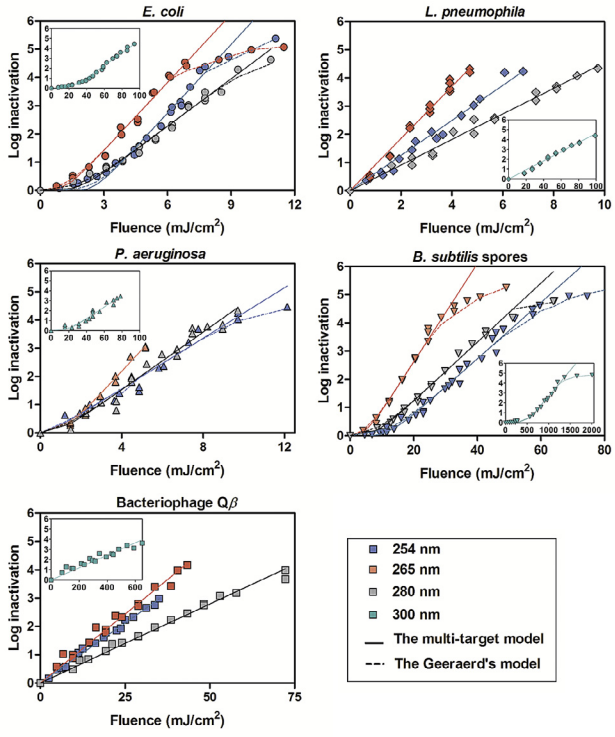

Fig. 2. Inactivation profiles and model fittings for tested microorganisms under exposures to LPUV and 265, 280-, and 300-nm UV-LEDs. Internal figures show the inactivation profile and model fitting for 300-nm UV-LEDs.

Table 1
The shoulder length (mJ/cm^2) of different species at different UV wavelengths. Errors indicate 95% confidence interval.

Microorganism	UV wavelength			
	254 nm	265 nm	280 nm	300 nm
E. coli	2.62 ± 0.09	1.25 ± 0.07	1.95 ± 0.12	23.4 ± 0.66
P. aeruginosa	0.52 ± 0.18	1.18 ± 0.04	1.01 ± 0.19	19.7 ± 1.11
L. pneumophila	~0	~0	~0	~0
Bacteriophage Qβ	~0	~0	~0	~0
B. subtilis spores	12.6 ± 0.51	4.96 ± 0.50	8.24 ± 0.66	481 ± 12.2

Introduction of the multi-target model to the fluence-response curves of all microorganisms as shown in Fig. 2 suggested that this model fitted well with the observed data, except for cases of *E. coli* and *B. subtilis* spores exhibiting sigmoidal curves. Because the multi-target model does not account for tailing, which may overestimate the effectiveness of UV-LEDs in the tailing region, another model covering both shoulder and tailing effects should be employed. The Geeraerd's model appeared to be suitable in the present study because this model not only uses a deterministic approach based on fitting, but also is supported by biological mechanisms in the background, such as possible factors affecting the shoulder (microorganims being clumped, damage re-synthesis ability, or difference in critical components) and tailing (existance of resistant sub-population, including adapted resistance).

As shown in Fig. 2, Geeraerd's model showed good fitting of not only the sigmoidal curves (*E. coli* and *B. subtilis* spores), but also curves with shoulders (*P. aeruginosa*) and linear curves of *L. pneumophila* and bacteriophage Qβ. Considering the goodness of curve fitting based on RMSE and R^2 as shown in Table 2 for the comparison between the multi-target and Geeraerd's model, the RMSE and R^2 values in linear fluence-response curves of *L. pneumophila* and bacteriophage Qβ for both models were equivalent at all wavelengths, and the sigmoidal curves for *E. coli* and *B. subtilis* spores were better characterized by Geeraerd's model at all wavelengths. For *P. aeruginosa* exhibiting fluence-response curves with a shoulder, the RSME of both models was similar. In conclusion, based on the results shown in Table 2, the Geeraerd's model covered all survival curve situations in this study.

3.2. Inactivation efficiency of UV-LEDs and LPUV

To compare the efficiency of UV inactivation at different wavelengths, inactivation rate constants calculated form a linear part for each microorganism are shown in Table 3.

3.2.1. 254 nm (LPUV)

Inactivation at this wavelength was effective against vegetative bacteria cells, particularly *E. coli*, *P. aeruginosa*, and *L. pneumophila*, with inactivation rate constants (k_{254} ± 95% confidence interval) of 0.81 ± 0.07, 0.45 ± 0.05, and 0.66 ± 0.03 cm^2/mJ, respectively. The range of k_{254} values for different *E. coli* strains reported in previous studies (Sommer et al., 2000; Hijnen et al., 2006; Rattanakul et al., 2014) was 0.44–0.91 cm^2/mJ, which is consistent with the results of the present study. Similarly, k_{254} for *L. pneumophila* was comparable to those in other studies (~0.7 cm^2/mJ) (Oguma et al., 2004; Cervero-Aragó et al., 2014), while *P. aeruginosa* appeared to be

Table 2
Comparison of goodness of fit between multi-target and Geeraerd's model among different microorganisms at different wavelengths.

	E. coli				*P. aeruginosa*				*L. pneumophila*				Bacteriophage Qβ				*B. subtilis* spores			
	RMSE		$^*R^2$		RMSE		$^*R^2$		RMSE		R^2		RMSE		R^2		RMSE		$^*R^2$	
	M	G	M	G	M	G	M	G	M	G	M	G	M	G	M	G	M	G	M	G
254 nm	0.373	0.157			0.287	0.217			0.188	0.188	0.978	0.978	0.072	0.072	0.994	0.994	0.497	0.181		
265 nm	0.853	0.174			0.106	0.117			0.173	0.173	0.984	0.984	0.116	0.116	0.979	0.979	0.349	0.240		
280 nm	0.170	0.144			0.250	0.252			0.154	0.154	0.985	0.985	0.123	0.123	0.987	0.987	0.269	0.128		
300 nm	0.150	0.141			0.244	0.233			0.146	0.146	0.986	0.986	0.291	0.291	0.912	0.912	0.683	0.137		

M = Multi-target model.
G = Geeraerd's model.
RMSE = Root square mean error.
R^2 is not applicable for non-linear regression.

Table 3
Inactivation rate constants at different UV wavelengths obtained from log-linear part on fluence-response curve. The *k* value shows the mean values, while error bars indicate 95% confidence interval of measurements. *n* shows the number of independent measurements.

	Inactivation rate constant, $k \pm 95\%$ CI (cm^2/mJ)				
	E. coli	*P. aeruginosa*	*L. pneumophila*	Bacteriophage Qβ	*B. subtilis* spores
254 nm	$(8.11 \pm 0.70) \times 10^{-1}$ ($n = 14$)	$(4.48 \pm 0.51) \times 10^{-1}$ ($n = 14$)	$(6.62 \pm 0.26) \times 10^{-1}$ ($n = 18$)	$(0.85 \pm 0.02) \times 10^{-1}$ ($n = 16$)	$(0.99 \pm 0.06) \times 10^{-1}$ ($n = 23$)
265 nm	$(8.05 \pm 0.55) \times 10^{-1}$ ($n = 17$)	$(7.74 \pm 0.49) \times 10^{-1}$ ($n = 16$)	$(8.60 \pm 0.51) \times 10^{-1}$ ($n = 18$)	$(0.98 \pm 0.06) \times 10^{-1}$ ($n = 18$)	$(1.74 \pm 0.15) \times 10^{-1}$ ($n = 13$)
280 nm	$(5.61 \pm 0.39) \times 10^{-1}$ ($n = 17$)	$(5.11 \pm 0.53) \times 10^{-1}$ ($n = 18$)	$(4.53 \pm 0.13) \times 10^{-1}$ ($n = 17$)	$(0.56 \pm 0.01) \times 10^{-1}$ ($n = 18$)	$(1.04 \pm 0.06) \times 10^{-1}$ ($n = 16$)
300 nm	$(0.63 \pm 0.04) \times 10^{-1}$ ($n = 20$)	$(0.59 \pm 0.06) \times 10^{-1}$ ($n = 15$)	$(0.48 \pm 0.03) \times 10^{-1}$ ($n = 17$)	$(0.06 \pm 0.004) \times 10^{-1}$ ($n = 18$)	$(0.05 \pm 0.006) \times 10^{-1}$ ($n = 10$)

more resistant than previously reported values of 0.95–1.3 cm^2/mJ, but the different strains used may account for the UV sensitivity difference (Clauß, 2006; Teksoy et al., 2011). Both Qβ and *B. subtilis* spores were highly UV resistant compared to the tested bacteria with k_{254} values of 0.08 ± 0.002 and 0.10 ± 0.006 cm^2/mJ, respectively; these values are comparable to previously reported values (Mamane-Gravetz et al., 2005; Rattanakul et al., 2014; Beck et al., 2015). The high UV resistance in *B. subtilis* spores may be related to the major UV-induced lesions in spores as spore photo-products rather than cyclobutane pyrimidine dimers and (6,4) photoproducts, major lesions in bacteria, and that spore photo-products can be repaired rapidly via specific mechanisms (Setlow, 2001). For Qβ and many viruses, factors, including their small size and host machinery-involving life cycle, may contribute to their high UV resistance.

3.2.2. 265 nm UV-LEDs

Inactivation rate constants of all tested microorganism were highest by inactivation with 265-nm UV-LEDs, except for *E. coli* whose rate constant was not significantly different from that at 254 nm ($p > 0.05$). The observed value of k_{265} (0.80 ± 0.06) for *E. coli* in the present study was higher than in previous studies (0.17–0.37 cm^2/mJ) (Chatterley and Linden, 2010; Oguma et al., 2013) and differences in experimental conditions and the shape of the inactivation profile may be involved. k_{265} values for *P. aeruginosa* and *L. pneumophila*, which were first reported in the present study, were 0.77 ± 0.05 and 0.86 ± 0.05 cm^2/mJ, respectively. There was no significant difference ($p > 0.05$) in k_{265} between *E. coli* and *P. aeruginosa*, and the k_{265} values for these species were slightly lower than that of *L. pneumophila.* Among the wavelengths tested, the 265-nm UV-LED achieved highest bacterial inactivation regardless of the bacterial species. This is because, as well-noted, UV absorbance of nucleic acid is highest at approximately 260 nm (Harm, 1980). Similarly, the k_{265} for *B. subtilis* spores and Qβ were higher than k_{254}, which is also attributable to the higher absorbance of nucleic acid at 265 nm.

3.2.3. 280 nm UV-LEDs

The UV absorbance of protein showed a relative peak at approximately 280 nm (Harm, 1980), and UV-induced protein damage may enhance microbial inactivation. However, as the UV absorbance of the genome decreases at this wavelength relative to that at 265 nm, k_{285} values for all microorganisms were also decreased to 0.56 ± 0.04 cm^2/mJ for *E. coli*, 0.51 ± 0.05 cm^2/mJ for *P. aeruginosa*, 0.45 ± 0.01 × 10^{-1} cm^2/mJ for *L. pneumophila*, 0.06 ± 0.001 cm^2/mJ for Qβ, and 0.10 ± 0.006 cm^2/mJ for *B. subtilis* spores. At 280 nm, Qβ and *B. subtilis* spores were more UV-resistant than bacteria, as was the case at 265 nm. Furthermore, inactivation by 280-nm UV-LED showed lower effectiveness than that by 254-nm LPUV in *E. coli*, *L. pneumophila* and Qβ, but remained the same as that at 254 nm, particularly for *P. aeruginosa* ($p < 0.05$) and was slightly higher for *B. subtilis*. For Qβ, UV-induced protein damage may not be a dominant cause of inactivation at this wavelength, although a previous study demonstrated that UV-induced protein damage played an important role in virus inactivation (Eischeid and Linden, 2011). The number of protein components involved in the infection processes of Qβ is lower than those of enteric viruses, which may result in a lower contribution of protein damage to inactivation.

3.2.4. 300 nm UV-LEDs

Although UV absorbance of both genome and protein considerably decreases at 300 nm, the inactivation rate constants of tested microorganisms (k_{300}) were still observable. The k_{300} values for vegetative bacteria cells were lowest among the other wavelengths. Similarly, k_{300} values for *B. subtilis* spores and Qβ were lowest among the wavelengths tested. These data are consistent with those of a previous study that tested the efficiency of UV-LEDs at 310 nm, demonstrating low but observable inactivation against *E. coli* (Oguma et al., 2013).

The present study showed that *E. coli* was more sensitive to UV than were the pathogenic bacteria, *P. aeruginosa* and *L. pneumophila* at all wavelengths. This poses a fundamental question regarding relevance of adopting *E. coli* as a surrogate for water-borne pathogenic bacteria for UV disinfection. This study also revealed that compared to conventional LPUV (254 nm) and other UV-LEDs wavelengths, inactivation of pathogenic and surrogate microorganisms by 265-nm UV-LEDs showed the best results based on the

Table 4
Electricity consumption per 3-$\log_{10}$ inactivation ($E_{E,3}$). Data indicate mean values of 3 independent measurements and error indicates 95% confidence interval of measurement.

	Electricity consumption per 3-$\log_{10}$ inactivation, $E_{E,3}$ ± 95% CI (kWh/m^3)				
	E. coli	*P. aeruginosa*	*L. pneumophila*	Bacteriophage Qβ	*B. subtilis* spores
254 nm	$(0.99 \pm 0.03) \times 10^{-2}$	$(1.08 \pm 0.06) \times 10^{-2}$	$(0.65 \pm 0.02) \times 10^{-2}$	$(4.86 \pm 0.11) \times 10^{-2}$	$(6.45 \pm 0.16) \times 10^{-2}$
265 nm	0.41 ± 0.01	0.39 ± 0.01	0.24 ± 0.004	2.02 ± 0.04	1.63 ± 0.06
280 nm	0.17 ± 0.01	0.17 ± 0.01	0.15 ± 0.002	1.11 ± 0.02	0.83 ± 0.02
300 nm	1.22 ± 0.03	1.22 ± 0.05	0.96 ± 0.02	7.44 ± 0.28	17.4 ± 1.29

fluence-based inactivation rate constants.

3.3. Electrical energy efficiency

Selection of UV-LEDs at different wavelengths based solely on inactivation rate constants can generate misleading results. Electrical energy efficiency is another factor involved in making an economically reasonable decision. In this study, electrical energy consumption per 3-$\log_{10}$ inactivation ($E_{E,3}$) was considered for all tested microorganisms, as the fluence-response curves of *E. coli*, *P. aeruginosa*, and *B. subtilis* spores were non-linear.

Table 4 shows the values of $E_{E,3}$ for all microorganism at different UV wavelengths. $E_{E,3}$ for tested microorganisms at 254 nm (LPUV) were 0.006–0.064 kWh/m^3, which were lower than those of UV-LEDs at all wavelengths for all species. Notably, $E_{E,3}$ of LPUV for Qβ and *B. subtilis* spores were approximately 5–10-fold higher than that for bacteria. Although 265-nm UV-LEDs provided higher inactivation rates than 254-nm LPUV, 265-nm UV-LEDs required approximately 25–40-fold more energy consumption for 3-$\log_{10}$ inactivation among all tested microorganisms. The $E_{E,3}$ of 265-nm UV-LEDs for bacterial species (*L. pneumophila*, *E. coli*, and *P. aeruginosa*) was lower than that for Qβ and *B. subtilis* spores, as was the case with LPUV at 254 nm. Additionally, 280-nm UV-LEDs consumed approximately half as much energy as 265-nm UV-LEDs for all microorganisms, definitely because of the difference in wall plug efficiency. The $E_{E,3}$ values of all tested microorganisms at 300 nm was highest compared to other wavelengths, showing the highest wall plug efficiency among the UV-LEDs tested. The low inactivation effectiveness resulted in high energy consumption to achieve a specific level of inactivation.

The $E_{E,3}$ values observed in this study for *E. coli* inactivation at 280 nm were lower than the value of 1.04 kWh/m^3, which was calculated based on the data reported by Beck et al. (2017). The lower energy consumption in the present study was mostly attributable to the difference in wall plug efficiency. Also, our results show that LPUV was more energy efficient than UV-LEDs at all wavelengths, as was reported previously (Austin et al., 2013; Beck et al., 2017). For UV-LEDs, 265 nm showed highest inactivation rate constants, while the 280-nm product was the most energy-efficient among the wavelengths tested. Energy consumption of 300 nm UV-LED was very high for all tested microbial species, particularly for *B. subtilis* spores requiring 17.4 kWh/m^3 for 3-$\log_{10}$ inactivation. Thus, energy consumption required for a certain level of inactivation may be a useful indicator for comparing UV light sources, including UV-LEDs.

4. Conclusions

UV-LEDs are effective for inactivating *P. aeruginosa*, *L. pneumophila*, and surrogate microorganisms in water. Among UV-LEDs with nominal peak emissions at 265, 280, and 300 nm, the 280-nm UV-LED is a good option for achieving a high inactivation rate constant and showed the lowest energy consumption for achieving 3-$\log_{10}$ inactivation in all microbial species tested. Our results can be used in the development of water disinfection systems with UV-LEDs.

Acknowledgements

This study was supported by the Japan Society for the Promotion of Science as the Grants-in-Aid for Scientific Research 26289181 and 17H03329, and Japan Science and Technology Agency as the Strategic International Research Cooperative Program. The authors are grateful to Nikkiso Giken Co., Ltd. for providing UV-LEDs and technical support for this study.

References

Adam, M.H., 1959. Bacteriophages. Wiley-Interscience, New York, USA.
Austin, O., Romelot, C., Rust, I., Hart, J., Jarvis, P., MacAdam, J., Parsons, S.A., Jefferson, B., 2013. Evaluation of a UV-light emitting diodes unit for the removal of micropollutants in water for low energy advanced oxidation processes. Chemosphere 92 (6), 745–751.
Beck, S.E., Wright, H.B., Hargy, T.M., Larason, T.C., Linden, K.G., 2015. Action spectra for validation of pathogen disinfection in medium-pressure ultraviolet (UV) systems. Water Res. 70, 27–37.
Beck, S.E., Ryu, H., Boczek, L.A., Cashdollar, J.L., Jeanis, K.M., Rosenblum, J.S., Lawal, O.R., Linden, K.G., 2017. Evaluating UV-C LED disinfection performance and investigating potential dual-wavelength synergy. Water Res. 109, 207–216.
Bowker, C., Sain, A., Shatalov, M., Ducoste, J., 2011. Microbial UV fluence-response assessment using a novel UV-LED collimated beam system. Water Res. 45 (5), 2011–2019.
Bolton, J.R., Linden, K.G., 2003. Standardization of methods for fluence (UV dose) determination in bench-scale UV experiments. J. Environ. Eng. 129 (3), 209–215.
Bolton, J.R., Stefan, M.I., Shaw, P.S., Lykke, K.R., 2011. Determination of the quantum yields of the potassium ferrioxalate and potassium iodide-iodate actinometers and a method for the calibration of radiometer detectors. J. Photochem. Photobiol. A. Chem. 222 (1), 166–169.
Buse, H.Y., Lu, J., Ashbolt, N.J., 2015. Exposure to synthetic gray water inhibits amoeba encystation and alters expression of *Legionella pneumophila* virulence genes. Appl. Environ. Microbiol. 81 (2), 630–639.
Centers for disease control and prevention (CDC), 2013. Antibiotic Resistance Threats in the United States, 2013 (Atlanta, Georgia).
Centers for disease control and prevention (CDC), 2015. Surveillance for Waterborne Disease Outbreaks Associated with Drinking Water — United States, 2011–2012 (Atlanta, Georgia).
Cerf, O., 1997. Tailing of survival curves of bacterial spores. J. Appl. Bacteriol. 42, 1–9.
Cervero-Aragó, S., Sommer, R., Araujo, R.M., 2014. Effect of UV irradiation (253.7 nm) on free *Legionella* and *Legionella* associated with its amoebae hosts. Water Res. 67, 299–309.
Chatterley, C., Linden, K.G., 2010. Demonstration and evaluation of germicidal UV-LEDs for point-of-use water disinfection. J. Water Health 8 (3), 479–486.
Clauß, M., 2006. Higher effectiveness of photoinactivation of bacterial spores, UV resistant vegetative bacteria and mold spores with 222 nm compared to 254 nm wavelength. Acta Hydrochim. Hydrobiol. 34 (6), 525–532.
Demirjian, A., Lucas, C.E., Garrison, L.E., Kozak-Muiznieks, N.A., States, S., Brown, E.W., Wortham, J.M., Beaudoin, A., Casey, M.L., Marriott, C., Ludwig, A.M., Sonel, A.F., Muder, R.R., Hicks, L.A., 2015. The importance of clinical surveillance in detecting Legionnaires' disease outbreaks: a large outbreak in a hospital with a *Legionella* disinfection system–Pennsylvania, 2011–2012. Clin. Infect. Dis. 60 (11), 1596–1602.
Eischeid, A.C., Linden, K.G., 2011. Molecular indication of protein damage in adenoviruses after UV disinfection. Appl. Environ. Microbiol. 77 (3), 1145–1147.
Facile, N., Barbeau, B., Prévost, M., Koudjonou, B., 2000. Evaluating bacterial aerobic spores as a surrogate for *Giardia* and *Cryptosporidium* inactivation by ozone. Water Res. 34 (12), 3238–3246.
Geeraerd, A.H., Herremans, C.H., van Impe, J.F., 2000. Structural model requirements to describe microbial inactivation during a mild heat treatment. Int. J. Food Microbiol. 59, 185–200.
Harm, W., 1980. Biological Effects of Ultraviolet Radiation. Cambridge University

Press, New York, p. 216.
Hijnen, W.A.M., Beerendonk, E.F., Medema, G.J., 2006. Inactivation credit of UV radiation for viruses, bacteria and protozoan(oo)cysts in water; a review. Water Res. 40 (1), 3–22.
Mamane-Gravetz, H., Linden, K.G., Cabaj, A., Sommer, R., 2005. Spectral sensitivity of Bacillus subtillis spores and MS2 coliphage for validation testing of ultraviolet reactor for water disinfection. Environ. Sci. Technol. 39, 7845–7852.
Meena, D.K., Gerba, P.C., 2009. Risk assessment of *P. aeruginosa* in water. In: Whitarce, D.M. (Ed.), Reviews of Environmental Contamination and Toxicology, vol. 201. Springer, USA, pp. 71–115.
Mossel, D.A.A., Corry, J.E.L., Struijk, C.B., Baird, R.M., 1995. Essential of the Microbiology of Foods. Wiley, West Sussex, UK.
Muhammad, N., Sinha, R., Krishnan, E.R., Piao, H., Patterson, C.L., Cotruvo, J., Cumberland, S.L., Nero, V.P., Delandra, C., 2008. Evaluating surrogates for *Cryptosporidium* removal in point-of-use systems. J. Am. Water Works Assoc. 100 (12), 98–107.
Nicholson, W.L., Setlow, P., 1990. Sporulation, Germination and Outgrowth. Molecular Biology and Methods for *Bacillus* (Pp. 391–418). Wiley, New York, USA.
Oguma, K., Katayama, H., Ohgaki, S., 2004. Photoreactivation of *Legionella pneumophila* after inactivation by low- or medium-pressure ultraviolet lamp. Water Res. 28, 2757–2763.
Oguma, K., Kita, R., Sakai, H., Murakami, M., Takizawa, S., 2013. Application of UV light emitting diodes to batch and flow-through water disinfection systems. Desalination 328, 24–30.
Oguma, K., Rattanakul, S., Bolton, J.R., 2015. Application of UV light-emitting diodes to adenovirus in water. J. Environ. Eng. 142 (3), 04015082-1 – 04015082–6.
ÖNORM, 2001. Austrian National Standard: ÖNORM M573-1 E. 2001. Plants for Disinfection of Water Using Ultraviolet Radiation: Requirements and Testing, Part 1. Low-pressure Mercury Lamp Plants. Austrian Standards Institute, Vienna, Austria.
Rattanakul, S., Oguma, K., Sakai, H., Takizawa, S., 2014. Inactivation of viruses by combination processes of UV and chlorine. J. Water Environ. Tech. 12 (6), 511–523.
Setlow, O., 2001. Resistance of spores of *Bacillus* species to ultraviolet light. Environ. Mol. Mutagen 38 (2–3), 97–104.
Severin, B.F., Suidan, M.T., Engelbrecht, R.S., 1983. Kinetic modeling of UV disinfection of water. Water Res. 17 (11), 2312–2322.
Sharpless, C.M., Linden, K.G., 2005. Interpreting collimated beam ultraviolet photolysis rate data in terms of electrical efficiency of treatment. J. Environ. Eng. Sci. 4, S19–S26.
Sommer, R., Lhotsky, M., Haider, T., Cabaj, A., 2000. UV inactivation, liquid-holding recovery, and photoreactivation of Escherichia coli O157 and other pathogenic Escherichia coli strains in water. J. Food Prot. 63 (8), 1015–1020.
Teksoy, A., Alkan, U., Eleren, S.Ç., Topaç, B.Ş., Sağban, F.O., Başkaya, H.S., 2011. Comparison of indicator bacteria inactivation by the ultraviolet and the ultraviolet/hydrogen peroxide disinfection processes in humic waters. J. Water Health 9 (4), 659–669.
U.S. Environmental Protection Agency (USEPA), 2006. Ultraviolet Disinfection Guidance Manual for the Final Long Term 2 Enhanced Surface Water Treatment Rule. US Environmental Protection Agency, Washington, D.C.
World Health Organization (WHO), 2017. Global Priority List of Antibiotic-resistant Bacteria to Guide Research, Discovery, and Development of New Antibiotics (Geneva, Switzerland).